

Photostability studies of three new bicyclo-boron dipyrromethene difluoride dyes

Wade N. Sisk^{a,*}, Noboru Ono^b, Tomoko Yano^b, Mitsuo Wada^b

^a*Department of Chemistry, The University of North Carolina Charlotte, Charlotte, NC 28223, USA*

^b*Department of Chemistry, Faculty of Science, Ehime University, Matsuyama 790-8577, Japan*

Received 16 July 2002; received in revised form 20 August 2002; accepted 24 September 2002

Abstract

The photostabilities of three novel bicyclo-boron dipyrromethene difluoride dyes (bicyclo-BODIPY) in solution were investigated by measuring the fluorescence intensity as a function of accumulated 532 nm laser pulses. At 10^{-6} M concentration 2-butanone and methanol solutions of the novel bicyclo-BODIPY dyes 1 and 2 exhibited photodegradation half-lives within 25% of the photodegradation half-life for 1,3,5,7,8-pentamethyl-2,6,-di-*t*-butyl pyrromethene difluoroborate (PM-597). At 10^{-7} M the photostability of a 2-butanone solution of bicyclo-BODIPY 2 is only half that of PM-597. Bicyclo-BODIPY dyes 1 and 2 demonstrated maxima in the fluorescence vs. accumulated pulses plots, attributed to a fluorescent benzo intermediate produced by a retro Diels–Alder reaction.

© 2002 Elsevier Science Ltd. All rights reserved.

Keywords: Boron dipyrromethene difluoroborate; BODIPY; Photoluminescence; Photostability; Photo-oxidation; Solid-state dye laser

1. Introduction

This study investigates the photostability of three new BODIPY dyes containing bicyclo octadiene or septadiene units (Fig. 1). The photostabilities are compared with the commercially available 1,3,5,7,8-pentamethyl-2,6,-di-*t*-butyl pyrromethene difluoroborate (PM-597) (Fig. 2).

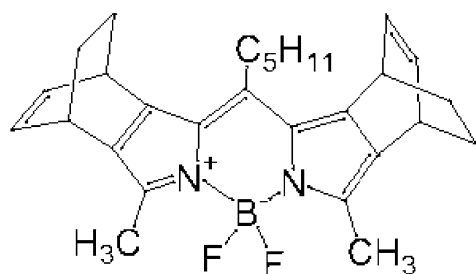
Boron dipyrromethene difluoroborate (BODIPY) dyes are suitable laser dyes due to their high fluorescence quantum yields and minimal triplet-triplet absorption over visible light excitation wavelengths [1,2]. Although several BODIPY dyes

are commercially available with lasing maxima in the 550–650 nm range, syntheses of new BODIPY dyes continue [3]. New BODIPY dyes vary in absorption/emission, solubility, fluorescence quantum yield, and photostability. Interest in the present bicyclo-BODIPY dyes stems from a preferred orientation in the molecular packaging in thin films attributed to their rigid three-dimensional structure [4].

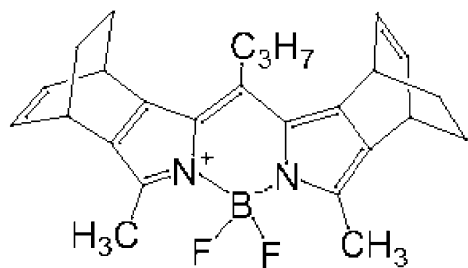
Photostability has taken on particular importance for solid-state dye lasers, in which the dye is dispersed in a polymer matrix [5–8]. This is due to the fact that the pump laser irradiates a restricted volume of dye molecules in solid-state dye lasers, whereas solution dye lasers typically employ dye circulation of a large volume of dye solution. We have previously investigated the photostability of

* Corresponding author. Tel.: +1-704-547-4433; fax: +1-704-687-3151.

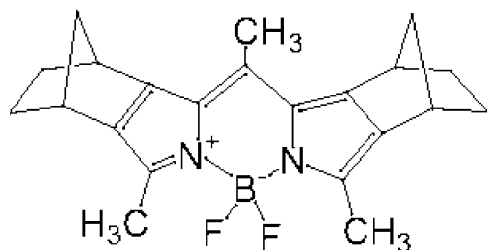
E-mail address: wsisk@email.uncc.edu (W. N. Sisk).



1

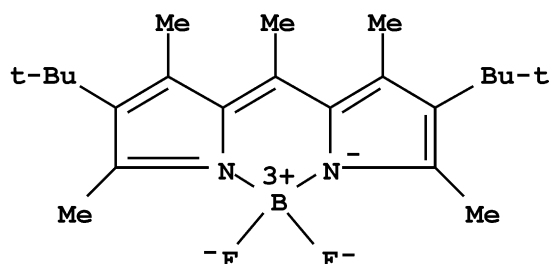


2



3

Fig. 1. Bicyclo-BODIPY dye structures.

Fig. 2. 1,3,5,7,8-Pentamethyl-2,6-di-*t*-butyl pyrromethene difluoroborate (PM-597).

methanol solutions of 1,3,5,7,8-pentamethyl-2,6-diethylpyrromethene difluoroborate (PM-567) with 532 nm laser irradiation, by monitoring the decrease in fluorescence at 595 nm with accumulated laser pulses [9]. That study and others have attributed photodegradation to singlet-oxygen mediated photo-oxidation [6,9,10]

2. Experimental

2.1. Sample preparation

Samples 1, 2, and 3 were prepared by a method previously reported [2]. As a typical procedure, sample 1 was prepared as follows. A solution consisting of 1.01 g (6.85 mmol) of 4,7-dihydro-4,7-ethano-1-methyl-2H-isoindole (prepared according to [11]), 1.91 ml (13.7 mmol) of hexanoyl chloride in 100 ml of CH_2Cl_2 was refluxed for 3 h. The reaction mixture was poured into 200 ml of hexane and precipitated solid was filtered. The solid was filtered and washed with hexane. This solid was dissolved in 150 ml of toluene and 1.77 ml (13.3 mmol) of triethylamine was added to the solution. Then 2.23 ml (14.03 mmol) of $\text{BF}_3\text{Et}_2\text{O}$ was added and heated at 80 °C for 30 min. After cooling to room temperature, the reaction mixture was filtered and the organic layer was washed with brine and dried with anhydrous sodium sulfate.

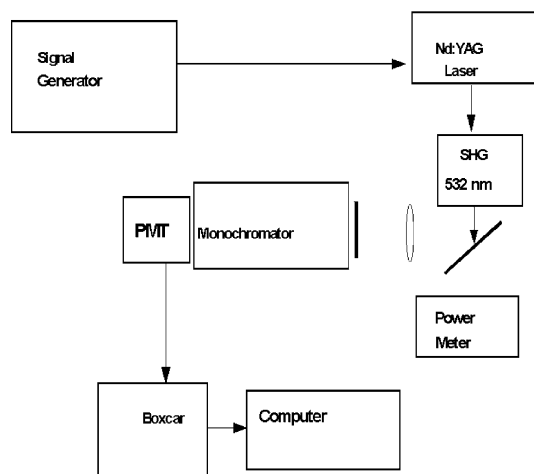


Fig. 3. Schematic diagram of experimental setup.

After evaporation of the solvents, the residue was subjected to column chromatography (silica gel) to give **1** (0.84 g, 55%). $^1\text{H-NMR}$ (CDCl_3) δ = 6.52 (m, 2H), 4.22 (m, 2H), 3.87 (m, 2H), 3.07 (t, J = 7.3 Hz, 2H), 2.48 (s, 6H), 1.75 (m, 2H), 1.60–1.43 (m, 12H), 0.95 (t, J = 7.3 Hz). MS (EI, 20 eV) [mass, intensity (%)] 446 (M^+ , 12), 418 (8), 390 (100), 334 (11). UV–vis (CHCl_3) λ_{max} nm ($\log \epsilon$) 529 (4.82), 390 (4.02). Analysis: calculated for $\text{C}_{28}\text{H}_{33}\text{BF}_2\text{N}_2$: C, 75.34; H, 7.45; N, 6.28; found: C, 75.28, H, 7.50, N, 6.25. Other samples **2** and **3** were prepared in the same way. **2** (yield 74%): $^1\text{H-NMR}$ (CDCl_3) δ = 6.52 (m, 2H), 6.44 (m, 2H), 4.21 (m, 2H), 3.87 (m, 2H), 3.06 (t, J = 7.8 Hz), 2.49 (s, 6H), 1.78 (m, 2H), 1.60–1.43 (m, 8H), 1.15 (t, J = 7.8 Hz, 3H). MS 370 (M^+ , 90), 342 (8), 314 (100), 271 (13), 229 (33), 201 (65). UV–vis (CHCl_3) λ_{max} nm ($\log \epsilon$) 530 (4.78), 389 (3.97). Anal. calcd for $\text{C}_{26}\text{H}_{29}\text{BF}_2\text{N}_2 \cdot 0.25\text{H}_2\text{O}$: C, 73.79; H, 7.03; N, 6.61. Found: C, 73.82; H, 6.79; N, 6.58. **3** (yield, 70%). $^1\text{H-NMR}$ (CDCl_3) δ = 3.53 (m, 2H), 3.24 (m, 2H), 2.54 (s, 3H), 2.49 (s, 6H), 1.92 (m, 6H), 1.61 (m, 2H), 1.13 (m, 4H). MS 366 (M^+ , 8), 338 (12), 219 (100), 149 (14). UV–vis (CHCl_3) λ_{max} nm ($\log \epsilon$) 526 (4.87), 387 (4.16). Anal. calcd for $\text{C}_{22}\text{H}_{25}\text{BF}_2\text{N}_2 \cdot 0.2\text{H}_2\text{O}$: C, 71.45; H, 6.92, N, 7.58; found: C, 71.65; H, 6.85; N, 7.51. Melting points could not be determined to the onset of a retro-Diels–Alder reaction that occurred at higher temperatures [3].

Rose Bengal (Aldrich), methylene blue (Aldrich), rubrene (Aldrich), and AlQ_3 (Aldrich), lidocaine (Sigma), and laser dyes R590 and PM-597 (Exciton) were used as received.

2.2. Photoluminescence measurements

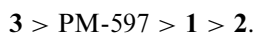
The experimental arrangement is shown in Fig. 3. Quartz cuvettes (1 cm) containing 0.70 ml of 10^{-6} – 10^{-7} M dye solution were irradiated by 0.5 cm diameter 532 nm laser light via the second harmonic of a Nd:YAG laser. Emission was monitored at 595 nm via a monochromator and photomultiplier tube (Hamamatsu R928 PMT). The amplified PMT response was averaged by a boxcar integrator. A pump-probe technique, previously described [9], was utilized in which the sample's fluorescence intensity was measured at

discrete time intervals for 10 s with a low laser fluence of $18 \text{ mJ cm}^{-2} \text{ pulse}^{-1}$. The irradiation occurred during the time between measurements utilizing a high pump laser fluence of $190 \text{ mJ cm}^{-2} \text{ pulse}^{-1}$. The low probe energy in addition to filters placed on the monochromator entrance slits, minimized scattered light contamination of the signal. The absence of a photoluminescent signal for a cuvette containing only solvent confirmed the insignificance of scattered light under the present experimental conditions.

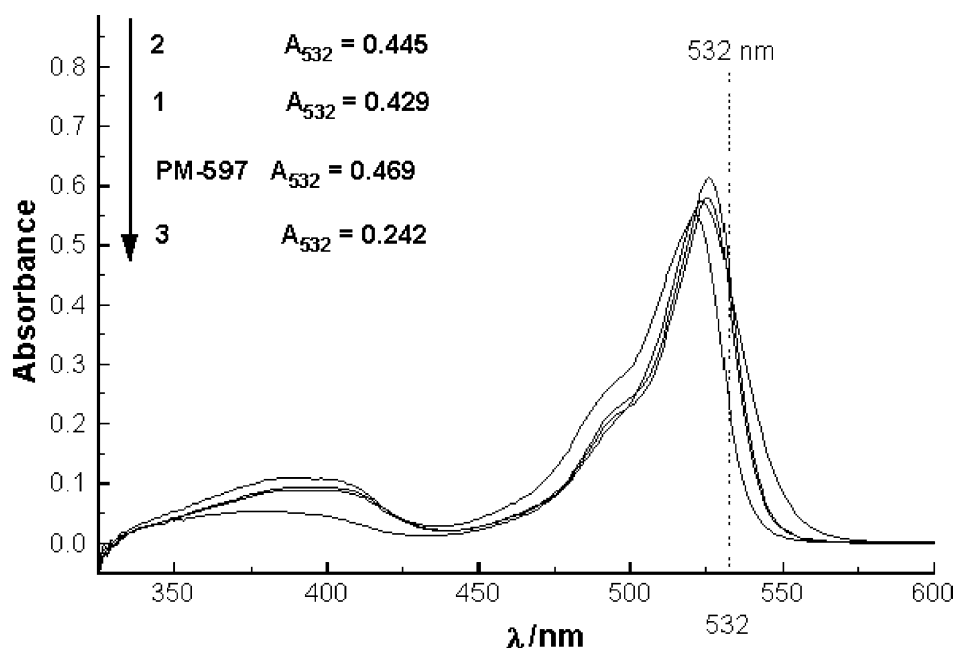
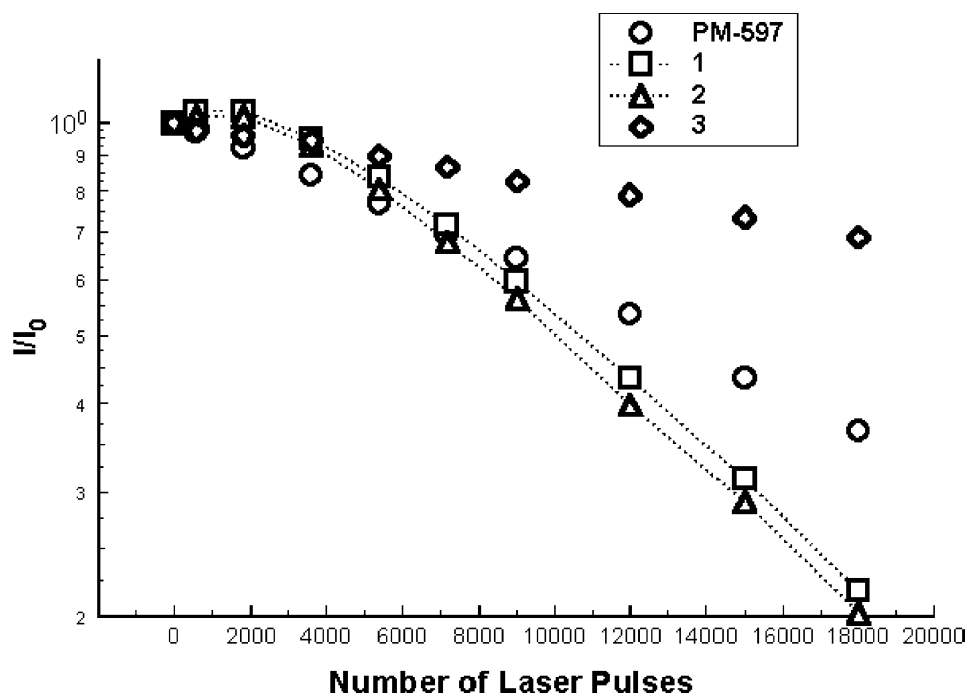
3. Results and discussion

In Fig. 4 the visible absorbance spectra of dye/2-butanone solutions are compared. Absorbance spectra of 8×10^{-6} M dye/2-butanone solutions were similar for PM-597, **1**, and **2**, but differed for **3** which was noticeably blue-shifted. The blue shift resulted in a lower 532 nm absorbance for **3** ($A_{532} = 0.242$) relative to **1** ($A_{532} = 0.429$), **2** ($A_{532} = 0.445$), and PM-597 ($A_{532} = 0.469$). A cuvette with pure solvent was placed in the reference beam of the spectrophotometer to account for 2-butanone absorption.

The results for 532 nm photodegradation of 8×10^{-6} and 8×10^{-7} M dye/2-butanone solutions are shown below in Figs. 5 and 6. The photostability trend for both concentrations is:



The high apparent photostability of **3** is attributed to its low 532 nm absorbance. Although singlet oxygen was not directly measured in this experiment, previous studies have suggested the singlet oxygen mediated photo-oxidation mechanism to be responsible for the photodegradation of pyrromethene dyes [6,9,10]. Thus, the apparent high photostability of **3** may be attributed to a much lower excited state dye concentration and subsequently a much lower singlet oxygen concentration. The absorbance of **1**, **2**, and PM-597 are similar and yet lower photostabilities, defined as photodegradation half-lives, are observed for **1** and **2**. This may be due to possibly higher singlet oxygen yields for **1** and **2** or higher singlet oxygen

Fig. 4. Visible absorbance of 8×10^{-6} M dye/2-butanone solutions.Fig. 5. Photoluminescence at 595 nm following accumulated 532 nm irradiation of 8×10^{-6} M dye/2-butanone solutions.

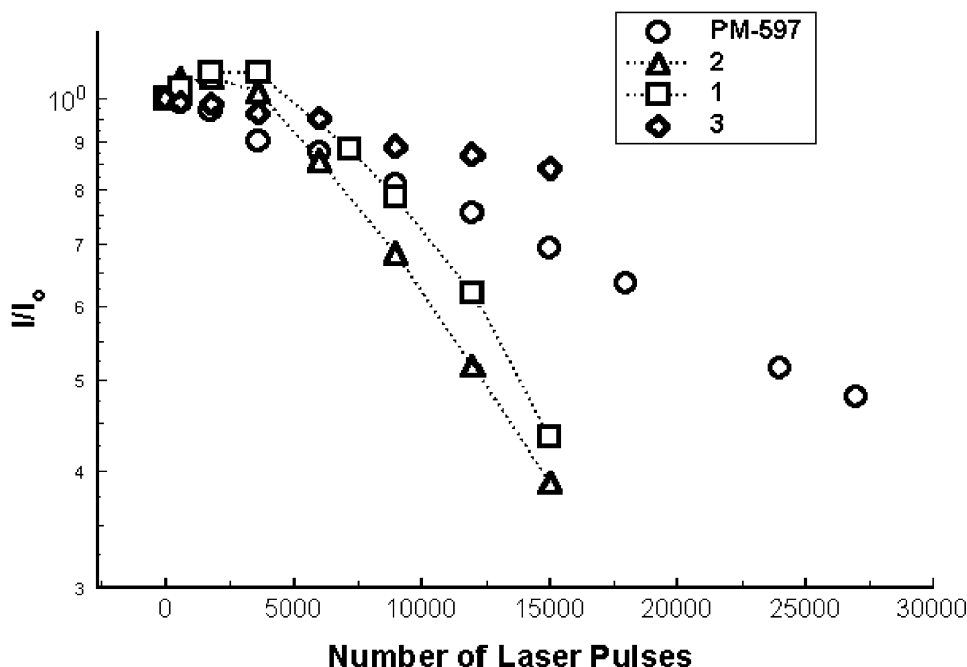


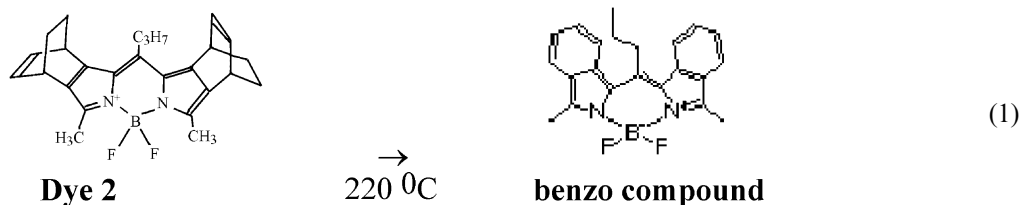
Fig. 6. Photoluminescence at 595 nm following accumulated 532 nm irradiation of 8×10^{-7} M dye/2-butanone solutions.

dye reaction yields (chemical quenching:physical quenching ratio). Investigations are underway to measure the $^1\text{O}_2(^1\Delta_g) \rightarrow ^3\text{O}_2(^3\Sigma_g^-)$ 1270 nm IR phosphorescence in order to address the above concern. The photostability difference of PM-597 and bicyclo-BODIPY dyes **1** and **2** is more pronounced for the lower concentration. The concentration dependence of photostability is consistent with that shown for previous studies of pyrromethene dyes: higher photostabilities exhibited by lower dye concentrations [9]. This concentration dependent photostability might be attributed to higher heat deposition for higher concentrations, due to the residual energy in red shifted fluorescent dye molecules and nonradiative dye molecules. Such a high heat deposition could increase the local temperature and preferentially increase the rate constants responsible for singlet oxygen dye chemical reactions. Thus, the Arrhenius increase in the photodegradation rate constants for higher concentrations may be responsible for lower photostability.

A maximum is observed in the photodegradation profiles for **1** and **2**, but not for **3** and PM-567. Initially it was thought that this rise and

subsequent decay was due to the formation and photodissociation of aggregates [12]: photodissociation of a nonfluorescent aggregate by initial laser pulses leading to more highly fluorescent free dye, followed by a decrease in the free dye concentration due to photo-oxidation with continual 532 nm irradiation. However, aggregate photodissociation cannot account for the concentration invariance of the appearance of maxima in Figs. 5 and 6, since aggregate formation would be less probable at lower concentrations. A more plausible explanation is that the maxima observed in the photodegradation profiles of **1** and **2** are possibly due to the initial formation of compound with higher fluorescence yields at 595 nm observation wavelengths (532 nm excitation), which is subsequently photo-oxidized into a compound with little or no fluorescence for accumulated 532 nm laser pulses.

The case for such a compound with possibly higher fluorescence yields at 595 nm is supported by recent work by Wada et al. [3]. In their investigation a retro Diels–Alder conversion of dye **2** into a fluorescent benzo compound was observed when **2** was heated at 220 °C under a reduced



atmosphere (10 Torr) [3]. This benzo compound absorbs and emits radiation at longer wavelengths (red-shifted) than dye **2**.

Although the fluorescent quantum yield of dye **2** ($\Phi = 0.80$) is much larger than the resultant benzo compound ($\Phi = 0.36$); the quantum yield restricted to 595 nm of this compound may exceed that of **2**. The reason for this is the fluorescence intensity at 595 nm is significantly lower than the maximum for both compounds. The relative fluorescence intensity, $I_{d\lambda}$, over an interval λ to $\lambda + d\lambda$ (determined by the monochromator slit width) is equal to the ratio of the fluorescence intensity over this interval to the fluorescence intensity integrated over all wavelengths. The fluorescence quantum yield over the observation wavelength interval is the product of the total quantum yield and the relative fluorescence intensity.

$$\Phi_{d\lambda} = \frac{I_{d\lambda}}{I} \times \Phi \quad (2)$$

Thus, the initial rise in fluorescence for the photodegradation profile of **2** may be explained by a relative fluorescent intensity ratio of the benzo compound-to-**2** that exceeds the 80:36 inverse quantum yield ratio. A similar explanation is proposed for dye **3**, since a maximum is observed in its photodegradation profile as well.

It is not clear how cumulative pulsed laser excitation produces the benzo compound. One possible mechanism is the direct photochemical conversion of **2/3** into the fluorescent compound via a retro Diels–Alder reaction. Another possibility is an indirect mechanism in which light absorption is followed by nonradiative energy transfer to heat the local environment leading to thermal initiation of the retro Diels–Alder reaction of **2/3** similar to that described by Wada et al. [3].

The role of the solvent on the relative photostability of PM-597 and the bicyclo-BODIPY dyes

was investigated for bicyclo-BODIPY **2**. The investigation was limited to bicyclo-BODIPY **2** since **3** did not possess adequate absorption at 532 nm to significantly photodegrade and the photodegradation behavior of **1** was similar to **2** in 2-butanone due to structural similarities. The 532 nm methanol photodegradation results (Fig. 7) are inverted with respect to 2-butanone: a slightly greater photostability displayed by **2** than PM-597. This may partially be attributed to the low absorbance for 10^{-6} M solutions of **2** ($A_{532} = 0.0509$) relative to PM-597 ($A_{532} = 0.0597$). As in 2-butanone a maximum is also observed for methanol solutions of **2**, but this is more pronounced than for the **2**-butanone solution.

The photostability half-lives are tabulated in Table 1. The half-lives of **1**, **2**, and PM-597 were determined by linear interpolation. The half-lives of **3** was determined by extrapolation of an exponential fit of photodegradation plots (Figs. 5 and 6). The long half-lives for **3** greatly exceeded the half lives of the other compounds attributed to the low absorption coefficient for **3**. The ratio of the

Table 1
Photostability half-lives

Sample	Concentration (M)	$\tau_{1/2}$ (pulses)
PM-597 ^a	8×10^{-6}	13,500
1 ^a	8×10^{-6}	10,800
2 ^a	8×10^{-6}	10,100
3 ^a	8×10^{-6}	34,000
PM-597 ^a	8×10^{-7}	25,000
1 ^a	8×10^{-7}	12,500
2 ^a	8×10^{-7}	13,900
3 ^a	8×10^{-7}	61,100
PM-597 ^b	1×10^{-6}	13,500
2 ^b	1×10^{-6}	16,500

^a 2-Butanone solvent.

^b Methanol solvent.

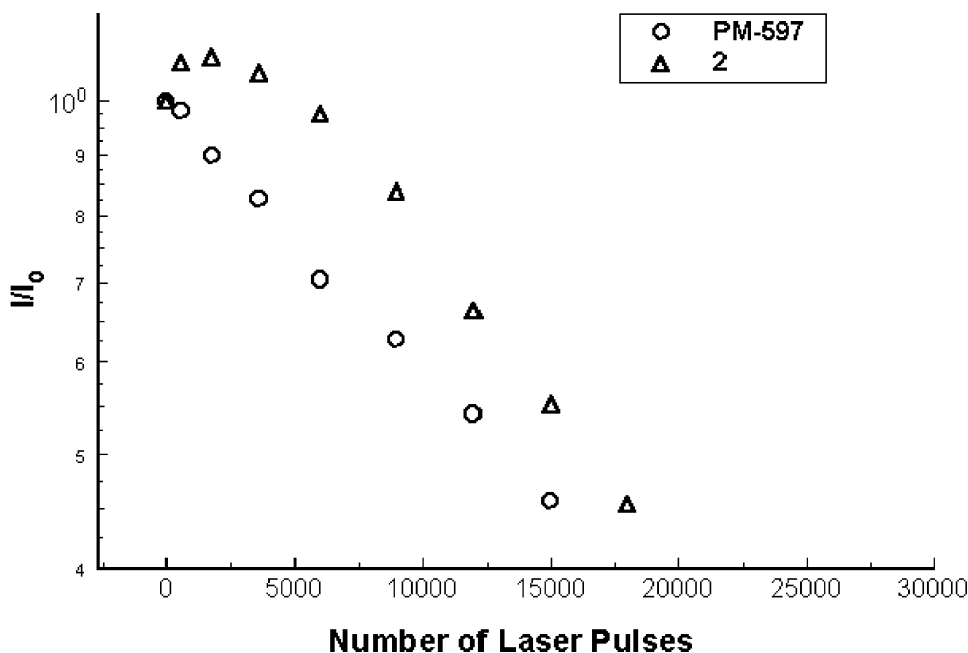


Fig. 7. Photoluminescence at 595 nm following accumulated 532 nm irradiation of 1×10^{-6} M dye/methanol solutions.

half-lives of 3 to the other compounds were 2.44–4.89 while the inverse of the absorption coefficient ratios were 1.77–1.94, thus a simplistic argument based on the number of absorbed photons is insufficient to completely explain the present observations, although it does give some indication for large differences in photodegradation rates. The half-lives also reflect the concentration and solvent dependence of photodegradation rates discussed above.

4. Conclusions

In solution the photostability of the novel bicyclo-BODIPY dyes are within a factor of 2 of the commercially available PM-597 dyes, thus no dramatic increases in photostability were observed in solution phase. One key difference between PM-597 and bicyclo-BODIPY photodegradation profiles is the maximum present in the bicyclo-BODIPY profiles indicative of the production of a fluorescent benzo compound via a retro Diels–Alder reaction. This suggests that strategy of adding antioxidants to enhance the photostability of

pyrromethene dyes might have limited effectiveness on the photostability of bicyclo-BODIPY dyes, since such antioxidants are not expected to suppress the retro Diels–Alder reaction [9]. Such studies are currently underway. Additional studies are planned to investigate the photostability and photoconductivity of the bicyclo-BODIPY thin films in which the molecular stacking may play a role. These investigations will impact the feasibility of solid-state organic photonic devices based on such bicyclo-BODIPY dyes.

References

- [1] Pavlopoulos TG, Shah M, Boyer JH. *Appl Opt* 1988; 27:4998.
- [2] Pavlopoulos TG, Boyer JH, Shah M, Thangaraj K, Soong ML. *Appl Opt* 1990;29:3885–6.
- [3] Wada M, Ito S, Uno h, Murashima T, Ono N, Urano T, et al. *Tetrahedron Lett* 2001;42:6711–3.
- [4] Long TM, Sager TW. *Adv Mater* 2001;13:601.
- [5] Hermes RE, Allik TH, Chandra S, Hutchinson JA. *Appl Phys Lett* 1993;16:877–9.
- [6] Rahn MD, King TA, Gorman AA, Hamblett I. *Appl Opt* 1997;36:5862–71.

- [7] Costela A, Garcia-Moreno I, Barroso J, Sastre R. *Appl Phys B* 2000;70:367–73.
- [8] Sardar DK, Yow RM, Mayo MLJ. *Appl Phys* 2001; 89:7739.
- [9] Mackey M, Sisk WN. *Dyes and Pigments* 2001;51:79–85.
- [10] Jones IIG, Klueva O, Kumar S, Pacheco D. *Solid State Lasers X SPIE* 2001:4267.
- [11] Ito S, Ochi N, Mujrashima T, Uno H, Ono N. *Heterocycles* 2000;52:399.
- [12] Allen NS, McKellar JF. *Photochemistry of dyed and pigmented polymers*. London: Applied Sciences; 1980.